Semiautomatic Detection of Microbubble Ultrasound Contrast Agent Destruction Applied to Definity® Using Support Vector Machines

Alexander Haak, Roberto Lavarello and William D. O'Brien, Jr.
Bioacoustics Research Laboratory
Department of Electrical and Computer Engineering
University of Illinois at Urbana-Champaign
Urbana, IL 61801 USA
Email: ahaak@uiuc.edu

Benjamin Castaneda
Rochester Center for Biomedical Ultrasound
Department of Electrical and Computer Engineering
University of Rochester
Rochester, NY 14623 USA

Abstract— **For different applications such as imaging, drug delivery, and tissue perfusion measurement, it is necessary to know the inertial cavitation (IC) threshold of ultrasonic contrast agent (UCA) microbubbles. Even though the influence of the incident acoustical pressure, frequency and pulse duration (PD) in the regime of the microbubble's response is well established, the investigation of the IC threshold is essential for the accuracy of some measurement techniques and for ultrasound safety. The goal of our work was to find the IC threshold for the FDA-approved UCA Definity®. The dependency of the threshold on the peak rarefactional pressure and PD of an incident tone-burst was investigated. The experiments performed to estimate IC thresholds yield a large amount of data to be classified in the five following classes: Noise, Oscillation, Collapse, Multiple Bubbles and Unknown. A reduction of the manually to classified data was reduced by using a semiautomatic algorithm in order to achieve a low variance in the IC estimates. Further more significant features to distinguish between classes were found and tested. The development of a heuristic algorithm to detect events of thee class Collapse was not successful due to the fact that the classes were overlapping and some signals could not be classified to a single class. Therefore, a semiautomatic algorithm using support vector machines was developed.**

I. Introduction

Ultrasound contrast agents are small, stabilized microbubbles (diameter $< 10\ \mu$m) that are used for several ultrasonic therapy and imaging applications. There are three different regimes (linear, nonlinear, and inertial cavitation (IC)) of microbubble responses to an incident ultrasound field. One of the earliest applications, using the linear regime, was the contrast enhancement of blood vessels in ultrasonic images due to the good ultrasound scattering qualities of the microbubbles [1]. Later, several image techniques were developed to measure blood perfusion, blood volume or blood velocity rates in tissue [2]. These techniques require the UCA destruction threshold to be known in order to avoid false measurements due to unintentional modification of the UCA concentration. The knowledge of UCA destruction threshold is also fundamental for targeted drug and gene delivery as well for safety reasons.

Several techniques have been developed using noise emission from microbubble destruction measured by a passive cavitation detector (PCD) to estimate UCA destruction thresholds. The use of high-speed cameras are currently the reference method to determine UCA destruction thresholds [3], but the expensive equipment limits its accessibility and is not usable for in vivo studies. Thus, we report on a technique using post-excitation broadband signals to identify microbubble destruction. These signals are linked to IC of bubbles released after UCA shell rupture. This technique has the advantage that the inertial collapse and rebound signals are not contaminated by nonlinear spectral contents from other sources [4].

The PCD measurements could be classified in five different classes (Noise, Oscillation, Collapse, Multiple Bubbles and Unknown) with unique patterns. However, we are interested in determining the relative number of collapses depending on peak rarefactional pressure, frequency and PD based on PCD measurements. Therefore large data sets need to be inspected for collapse events in order to achieve a reasonable low variance of the threshold estimate. In order to reduce the number of samples to be manually inspected, Support Vector Machine (SVM) classifiers were applied to pre-classify the data. SVMs are binary classifier, trained on supervised data and were successfully used for different pattern recognition problems such as content based image retrieval [5] and facial expression classification [6]. Furthermore, to distinguish between collapse and non collapse events, appropriate features need to be identified. Receiver operator characteristic (ROC) analysis was used to select the most significant features based on their discrimination properties.

II. Methods and Materials

A. Contrast Agent

For all experiments the FDA-approved contrast agent Definity® was used. The UCA is a lipid shell microbubble that contains Octafluoropropane (C_3F_8) gas. The manufacture's vials have a maximum concentration of 1.2 x 10^{10} microbubbles/mL. Before use, Definity® was activated using Vialmix™ [7]. The mean diameter of the microbubble distribution is between 1.1 and 3.3 μm, the maximum diameter is less than

20 μm and approximately 98% of the bubbles have a diameter less than 10 μm.

B. Experimental Setup

The PCD system described by Ammi et.al. [4] [8], consisted of two focused transducers (2.8 MHz driving and 13 MHz receiving transducers), was used to expose the UCA microbubbles and to record their scattered signals. The schematic layout of the experiment is shown in Fig. 1. In the tank was a weak solution of UCA that resulted in one microbubble in the confocal volume on average. The microbubbles were excited with the 2.8 MHz and the scattered signal was received by the 13 MHz transducer, amplified (44 dB), digitized (12-bit, 200 MS/s, Strategic Test digitizing board UF 3025, Cambridge, MA) and saved to a PC using Matlab® (The Math Works, Inc., MA) for off-line processing. For each PD (3, 5 or 7 cycle) one hundred PCD waveforms were acquired from each of thirteen peak rarefactional pressure levels (ranging from 1.7 to 3.6 MPa).

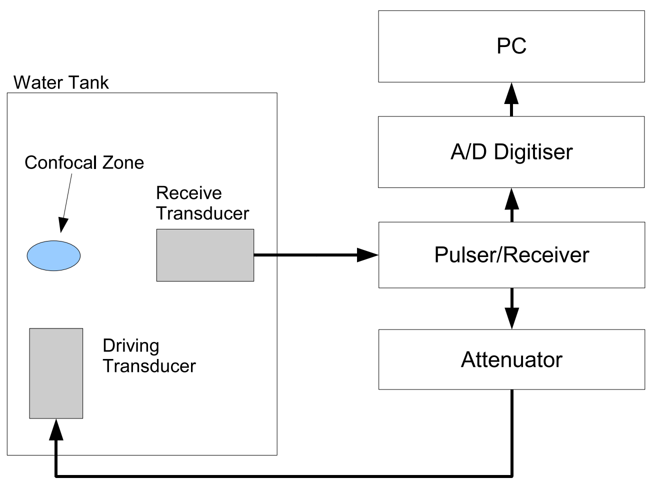

Fig. 1. Experimental setup of the passive cavitation detector.

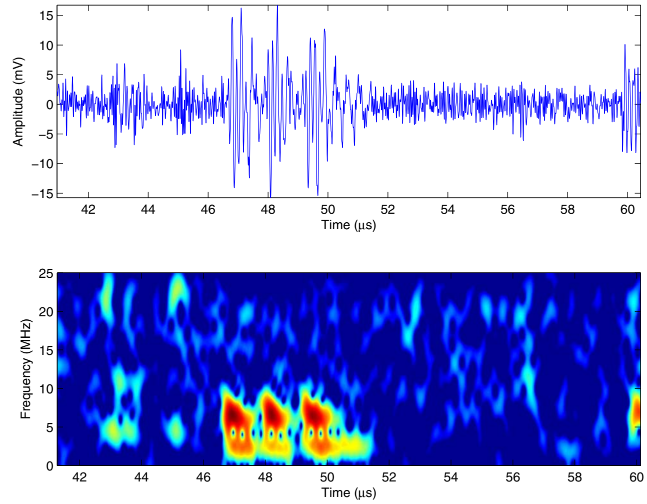

Fig. 2. An example of a waveform of the class Noise with signal artifacts.

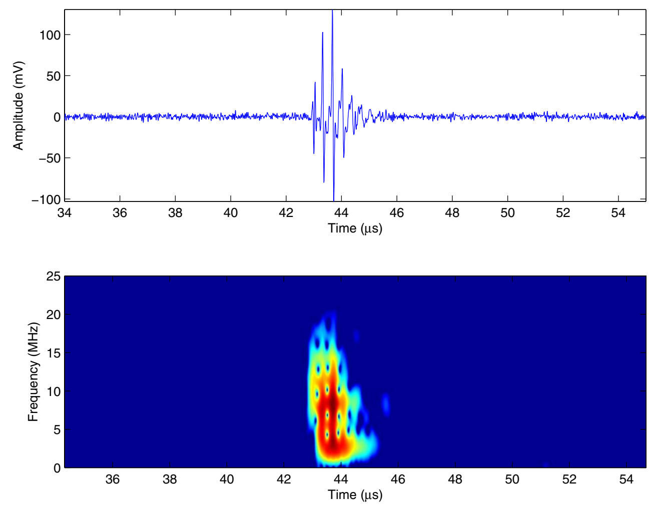

Fig. 3. An example of a waveform of the class Oscillation. A 2.8-MHz 3-cycle 2.9-MPa peak rarefactional pressure tone burst was used to excite the bubble.

C. Data Processing and Classification

The prototype data set was manually classified to train the SVM and test the accuracy of the algorithm. Deeper analysis of the measurements showed that the class boundaries were overlapping and some signals could not be subscribed to a single class. Therefore a fuzzy classification was used whereas every signal was weighted to all of the five classes introduced in Section I. These classes are described below:

1) Noise: Data acquired with no UCAs in the tank showed the presence of radiofrequency interference signals that could be incorrectly interpreted as generated by the contrast agents. Fig. 2 is a representative example for such a waveform. The signal content between 45 and 51 μs could possibly be interpreted as multiple, nonlinear oscillating microbubbles with fundamental and first harmonic modes.

2) Oscillation: Fig. 3 shows a representative PCD waveform from a single microbubble that was classified as Oscillation. The content of the waveform between approximately 43 and 46 μs corresponds to the PCD response of the microbubble echo. In the spectrogram, the fundamental mode, at approximately 3 MHz, and the harmonic modes, at 6, 9, 12 and 15 MHz, are visible. The harmonic modes may have been generated both by nonlinear bubble dynamics and nonlinear propagation of the exciting pulse and echo [4]. There was no acoustic emission after the end of the driving pulse.

3) Collapse: Fig. 4 shows a representative PCD waveform from a single microbubble that was classified as Collapse. The principal response of the microbubble between 42 and 45 μs looks similar to the waveforms of the class Oscillation. Frequency bands corresponding to the fundamental and harmonic modes are present in the spectrogram. Broadband signals (rebounds) with a frequency band between approximately 3 and 22 MHz appear after the principal response at 46 μs and 48 μs. This post-principal response feature indicates that inertial cavitation occurred [4].

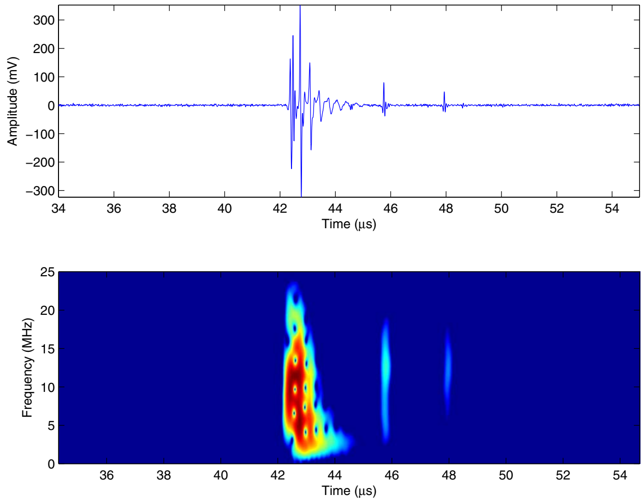

Fig. 4. A representative waveforms of the class Collapse. A 2.8-MHz 3-cycle 2.75-MPa peak rarefactional pressure sinusoidal tone burst was used to excite the bubble.

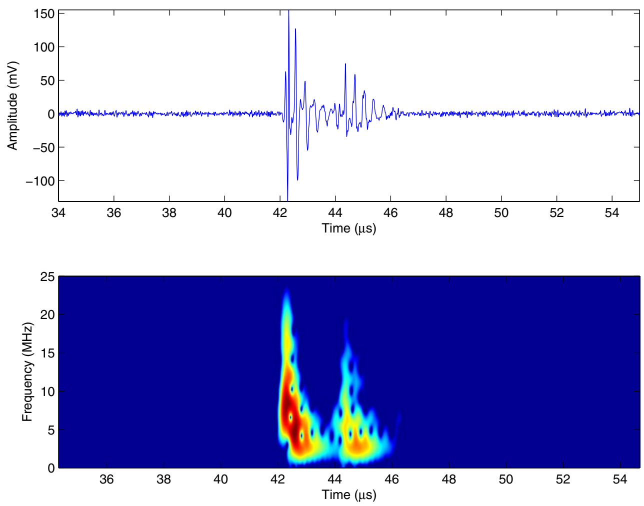

Fig. 5. An example of a waveform with two microbubbles of the class Oscillation. One of the responses is between 42 and 44 μs and the other between 44.8 and 45.8 μs. A 2.8-MHz 3-cycle 2.68-MPa peak rarefactional pressure sinusoidal tone burst was used to excite the bubbles.

4) Multiple Bubbles: Waveforms of the class Multiple Bubbles show characteristics of both Oscillation and Collapse classes, but the PCD response contains signals of multiple microbubble responses. In Fig. 5 there are two microbubble responses, one between 42 and 44 μs and the other between 44.8 and 45.8 μs, each with features of the class Oscillation.

5) Unknown: All waveforms that could not be classified as Noise, Oscillation, Collapse or Multiple Bubble were marked as Unknown.

D. Support Vector Machines

In this work the program SVM*light* was used to perform all pre-classification [9]. A SVM is a binary maximal margin classifier which was proposed by Vapnik et.al. [10]. To overcome problems of noise and non-separability a soft margin

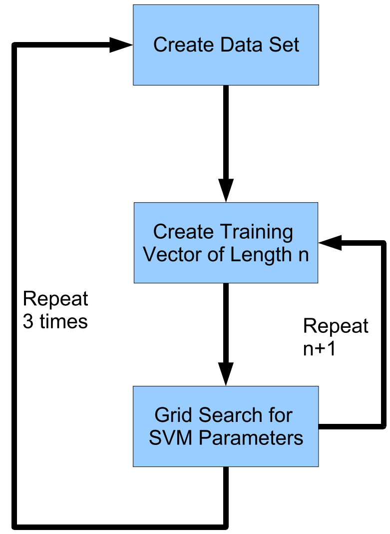

Fig. 6. Algorithm for estimation of the optimal feature and SVM parameter (σ and C) combination.

SVM using slack variables was introduced [11]. The scalar inner products were calculated using a nonlinear Gaussian Radial Basis kernel functions. The SVM classifiers required the selection of two independent parameters whose optimal values were obtained using a grid search method.

E. Feature Selection and SVM Training

For the SVM training and classification features with good discrimination properties needed to be found. From the prototype data set, signal that belonged to at least 70 % to the class Collapse were used as positive objects for the SVM training. An equal number of negative objects were randomly chosen from signals that did not belong to 70 % of the class Collapse. The prototype data set was equally divided into training and test data. The test set was used to test the classification performance of the algorithm and the training set was used to develop it. A total of 99 different features were automatically selected from the measured data belonging to the training set and tested for discrimination significance using the area under the ROC curve criterion. The classification performance of the SVM can be improved by using a larger number of features, but the performance of the classifier degrades when using too many features with bad discrimination properties. To find the optimal combination of good features and SVM Parameters (σ and C) the procedure shown in Fig. 6 was performed. First, the feature with the best discrimination property was used and the optimal SVM parameters were found using cross validation and grid search. Then, the two best features were used and the classification performance was tested. More and more features were added to the input vector of the SVM until the classification performance dropped.

F. Semi-Automatic Algorithm

After the SVM was trained data sets could be classified. Fig. 7 shows the layout of the algorithm. First, features were

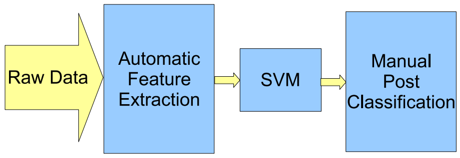

Fig. 7. Block diagram semi-automatic Algorithm for Collapse detection. Features were extracted from the raw data and followed by a pre-classification performed by a SVM. A manually post-classification was performed to increase the overall accuracy.

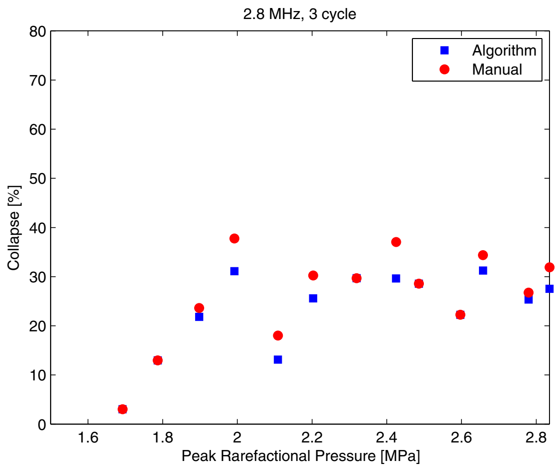

Fig. 8. Relative IC thresholds of Definity® for the 2.8 MHz, 3 cycle PD data set vs peak rarefactional pressure. The blue squares represent the results of the semi-automatic algorithm the red dots correspond to the results of the manually classified test data set.

extracted from the raw data and a trained SVM performed a pre-classification. The output margin of the SVM was as a confidence criteria used and signals with a low confidence were manually post-classified in order to achieve a better overall performance.

III. Results and Discussion

The relative IC threshold was estimated for the 2.8 MHz prototype dataset. In Fig 8 the threshold vs. peak rarefactional pressure is shown for 3 cycle PD. The relative error between algorithm and manual classification was around 3 %.

The estimated number of Collapses was divided by the number of events that had higher RMS amplitude (>10 mV) in the window corresponding to the time of flight for every pressure level. This canceled out every dependency on concentration fluctuations of UCA in the tank. With the SVM algorithm a true positive rate of at least 80 % was achieved whereas a false positive rate was no higher than 8 %. The amount of data to be manually classified was reduced by 80%. The ratio of IC events to non-IC events ranged from 30% to 5%.

The ROC analysis showed that in general the amplitude of five following peaks after the maximum of the radiofrequency signal had the best discrimination properties for the class Collapse. A cluster analysis may help to identify redundancies and distributions of the different features.

IV. Conclusion

The relatively simple technique of the PCD was applied to the lipid shelled UCA Definity®. A semi-automatic algorithm with significant classification accuracy between IC and non-IC events was developed. Through the supervised trained SVM a post-classification was performed which led to a reduction of data that needed to be classified manually, thus providing the possibility to inspect large data sets for threshold estimations.The IC threshold for Definity®, using the post-excitation signal rebound as a criteria [4], was determined at 2.8 MHz.

Acknowledgment

This work was supported in part by NIH Grant R37EB02641 and in part by Beckman Institute for Advanced Science and Technology's Research Initiative in Targeted Contrast and Therapeutic Agents for Molecular Biomedical Imaging.

References

[1] A. P. Miller and N. C. Nanda, "Contrast echocardiography: New agents", *Ultrasound Med. Biol.*, vol. 30, pp. 425-434, 2004.
[2] K. Wei, A. R. Jayaweera, S. Firoozan, A. Linka, D. M. Skyba, and S. Kaul, "Quantification of myocardial blood flow with ultrasound-induced destruction of microbubbles administered as a constant venous infusion", *Circulation*, vol. 97, pp. 473-483, 1998.
[3] J. E. Chomas, P. Dayton, D. May, and K. Ferrara,"Threshold of fragmentation for ultrasonic contrast agents", *J. Biomed. Opt.*, vol. 6, pp. 141-150, 2001.
[4] A. Y. Ammi, R. O. Cleveland, J. Mamou, G. I.Wang, S. L. Bridal, and W. D. O'Brien, Jr., "Ultrasonic contrast agent shell rupture detected by inertial cavitation and rebound signals", *IEEE Trans. Ultrason., Ferroelect., Freq. Contr.*, vol. 53, pp. 126–136, 2006.
[5] D. Tao, X. Tang, X. Li, and X. Wu, "Asymmetric bagging and random subspacing for support vector machines-based relevance feedback in image retrieval", *IEEE Trans. Pattern Analysis and Machine Intelligence*, accepted for publication.
[6] J. Ghent and J. McDonald, "Facial expression classification using a one-against-all support vector machine", *Proceedings of the Irish Machine Vision and Image Processing Conference*, 2005.
[7] Bristol-Myers Squibb Medical Imaging, DEFINITY® Vial for (Perflutren Lipid Microsphere) Injectable Suspension 515188–0904, *prescribing info* 2004.
[8] A. Haak and W. D. O'Brien, Jr., "Detection of microbubble ultrasound contrast agent destruction applied to Definity", *Proceeding of the International Congress on Ultrasound*, Paper Number 1719. Available at http://papers.icultrasonics.org/, 2007.
[9] T. Joachims, Making large-Scale SVM Learning Practical. Advances in Kernel Methods - Support Vector Learning, B. Schlkopf and C. Burges and A. Smola (ed.), *MIT-Press*, 1999.
[10] B. E. Boser, I. Guyon and V. Vapnik, "A training algorithm for optimal margin classifiers", *Computational Learning Theory*, pp. 144–152, 1992.
[11] V. N. Vapnik, The Nature of Statistical Learning Theory. *Springer*, 1995.